X Encontro Brasileiro sobre Adsorção
27 a 30 de Abril de 2014
Guarujá - SP

CO_2 ADSORPTION USING POLYETHYLENIMINE-MAGADIITE

Rômulo B. Vieira[1*] and Heloise O. Pastore[1]

[1]Micro and Mesoporous Molecular Sieves Group, Inorganic Chemistry Department, University of Campinas
Rua Monteiro Lobato, 270 – CEP: 13083-861 – Campinas – SP – Brazil.
Phone: (19) 3521-3017 – Fax: (19) 3521-3023 – *Email: gpmmm@iqm.unicamp.br

ABSTRACT. Magadiite and organo-magadiite were impregnated with polyethylenimine (PEI) for CO_2 adsorption and, after characterizations, revealed not only the presence of PEI but also its interaction with CO_2 at low temperatures. The thermal stability of sorbents was confirmed by thermogravimetry experiments while their adsorption capacity was evaluated by CO_2-TPD experiments. Two kinds of PEI are present in the sorbent, one exposed PEI layer that is responsible for higher CO_2 adsorption because its sites are external and another one, bulky PEI, capable of low CO_2 adsorption due to the internal position of adsorption sites. The contribution of the exposed PEI layer may be increased by a previous exchange of CTA^+, but the presence of the surfactant decreased the total adsorption capacity. MAG-PEI25 reached a maximum adsorption capacity of 6.11 mmol g^{-1} at 75 °C after 3 h of adsorption and followed the Avrami kinetic model.

KEYWORDS: magadiite; polyethylenimine; adsorption; carbon dioxide; Avrami.

1. INTRODUCTION

The technological changes that occurred in the eighteenth century, initiated by the industrial revolution, increased greenhouse gas emissions, specifically CO_2. In that period, CO_2 accumulated emissions were around 280 ppm and reach values up to 390 ppm nowadays (Choi *et al.* 2009).

Thereby, several methods to remove CO_2 involving chemical and physical processes were developed. Carbon capture and storage (CCS) is one of them and includes CO_2 adsorption, compression, transport and storage. In the case of power plants, it can be used in precombustion, postcombustion and oxycombustion conditions (Samanta *et al.* 2012). The use of monoethanolamine (MEA) and diethanolamine (DEA) is presently the technology industrially applied with efficiency, but it is very expensive because of the large amounts of solvent required, besides the large energy demand for regeneration of these liquid amines, corrosion problems, and loss of amines by evaporation or decomposition in power plants (Choi *et al.* 2009). Given these disadvantages, the utilization of solid sorbents offers advantages when compared with the use of liquid amines. These are: low energy requisition, no corrosion, and a reduced loss of sorbent and of separation steps at low CO_2 partial pressures (Choi *et al.* 2009). Furthermore, solids showed fast adsorption/desorption kinetics, large adsorption capacity, are regenerable and stable.

Xu *et al.* (2002) developed the molecular basket sorbent and obtained an adsorption capacity of 2.54 mmol g^{-1} at 75 °C and 50 wt % of polyethylenimine (PEI) impregnated in MCM-41 with an efficiency of 0.11.

The PEI is a polymeric amine which has been widely used in the preparation of these sorbents, mainly due to the large concentration of amine groups controlled by synthesis conditions, molecular weight, and a moduled 1°/2°/3° amines ratio (Von Harpe *et al.* 2000).

A major problem encountered in these sorbents is the access of CO_2 to the inner portions of pores or channels in which adsorption sites are located. In an attempt to reduce or eliminate the diffusion troubles, the layered materials, specifically the layered silicate known as magadiite, have been studied by our group. Magadiite [$Na_2Si_{14}O_{29}\cdot(5\text{-}10)H_2O$] is a hydrated layered silicate discovered in 1967 by Eugster (1967). The silicon atoms are in tetrahedral coordination to four oxygen atoms and the layer surface has negative charges and Si-OH groups which provide a high reactivity to the layer surface.

Magadiite may be used as inorganic support for polymers due mainly to the flexibility of interlayer space and the fact that adsorption sites will not be occluded in pores or channels, but distributed in the expandable interlayer space of silicate.

In this paper, a solid sorbent has been developed by the synthesis of magadiite and the modification through an ion exchange procedure with hexadecyltrimethylammonium bromide (CTAB) and impregnation with PEI. To our knowledge, no reports can be found in the literature about the application of layered silicates in CO_2 adsorption; therefore, this paper is the first that evaluates their use as sorbents for the CO_2 adsorption.

2. MATERIALS AND METHODS

2.1. Magadiite and organo-magadiite

The synthesis of magadiite was carried out according to Superti *et al*. (2007). Briefly, sodium metasilicate ($Na_2SiO_3\cdot5H_2O$) (0.14 mol) was dissolved in distilled water (13.89 mmol) and the pH was adjusted at 10.6-10.8 with concentrated HNO_3. A gel was formed and was aged for 4h at 74-76 °C. After that, it was transferred to a stainless steel autoclave lined with Teflon for the hydrothermal treatment for 66 h at 150 °C. The material was filtered, washed until pH 7.0, dried in air and named MAG.

The organo-magadiite was prepared by ion exchange performed by dispersing 1.0 g of magadiite in 100 mL of MiliQ water. Then, CTAB was added and the mixture was kept under magnetic stirring for 24 h at 50 °C. The general formula of magadiite is $Na_2Si_{14}O_{29}\cdot(5\text{-}10)H_2O$, and CTA^+ ions were exchanged at a CTA/Na molar ratio equal to 25%. Last, the material was washed until the end of foaming and dried in the air at room temperature. The material was named 25CTA-MAG.

2.3. Layered Solid Sorbent

The sorbent were prepared by the impregnation method described previously by Xu *et al.* (2012). First, the desired amount of PEI (Mn=800), was dissolved in 25 mL of methanol for 1 h. At the same time, MAG or 25CTA-MAG was dispersed in 100 mL of methanol for 1 h. After that, PEI solution was added dropwise under stirring to guarantee a good dispersion of the PEI on the layered silicates suspension. The solution was stirred for 24 h at 60 °C, and the solvent was removed from the mixture at 50 °C by rotoevaporation and the solid was dried at 100 °C overnight. The sorbents were named MAG-PEI-x and 25CTA-MAG-PEI-x, where x represents the loading of PEI as weight percentage in the sample. The final material was obtained as a white solid, which agglomerated with increasing concentration of PEI. The amounts of PEI used were between 10 and 25 %.

2.4. Characterization

To confirm the formation of the desired materials, X-ray diffraction (XRD) was performed in a Shimadzu XRD7000 apparatus with a Cu Kα = 1.5406 Å (40 kV, 30 mA) source. Slits of 5 mm were used for dispersion and convergence and 3° for exit. The measurements were obtained between 1.4 and 55° 2θ at room temperature at a scan rate of 2° 2θ min^{-1}. The basal spacing of the layered silicates was calculated by Bragg's law. Fourier transformed infrared spectroscopy (FTIR) using KBr pellets (0.25 wt %) was performed with the use of a Thermo Nicolet 6700 FTIR spectrophotometer equipped with a DTGS detector (resolution 4 cm^{-1}). Spectra

were collected in the range from 400 to 4000 cm^{-1} by accumulating 128 scans. ^{13}C SS NMR was measured in a Bruker 400 MHz Avance 400 spectrometer. The samples were spun at 10 kHz in a zirconia rotor, and adamantane ($C_{10}H_{16}$) was used as reference. Elemental analyses of carbon, hydrogen, and nitrogen (CHN) were performed in a PerkinElmer 2400 Series II CHNS/O Elemental Analyzer. Thermogravimetric analysis was performed in a Setaram Instrument SETSYS 16/18 Evolution TGA with an alumina pan under He atmosphere (16 mL min^{-1}) in a temperature range from 20 to 1000 °C at a heating rate of 10 °C min^{-1}.

2.5. CO_2-TPD Experiments

The experiments were performed on a Quantachrome CHEMBET-3000 TPD/TPR instrument equipped with a TC detector. Approximately 100 mg of sorbent was placed in a U-shaped quartz reactor, heated to 150 °C at a rate of 10 °C min^{-1} and held at this temperature for 3 h under a He flow (30 mL min^{-1}). Then, the temperature was reduced to 75 °C, and CO_2 (5 vol. % in He) flow (20 mL min^{-1}) contacted the sorbent for 3 h. After that, the sample was submitted to a He flow (20 mL min^{-1}) for 1 h and the temperature decreased to 30 °C. The CO_2 desorption was carried out between 30 and 150 °C at a rate of 10 °C min^{-1}, and the CO_2 adsorption capacity was calculated on the basis of desorption by the external calibration method.

2.6. Avrami Kinetic Model

A kinetic model was applied in order to obtain more details of the kinds of interactions that occur between CO_2 and alkyl amine groups present in the branching PEI. Some works in the literature (Wang *et al.* 2012) used the Avrami kinetic model to describe the adsorption of CO_2 on mesoporous silica modified with alkyl amines. Considering that CO_2 desorption is the decomposition of alkylammonium alkylcarbamate, it may be fitted by the Avrami model (Kinefuchi *et al.* 2008) and these observations allow the use of this kinetic model in CO_2 desorption studies. The desorption experiments were fitted with the Avrami kinetic model showed in Eq. 01.

$$q_t = q_e[1-\exp(-(k_A t)^{n_A})] \quad (01)$$

where q_t represents the amount of CO_2 desorbed at time t, q_e is the total amount of CO_2 desorbed (adsorbed at equilibrium), k_A is the Avrami kinetic constant, and n_A is the Avrami exponent and is related to the existence of different reaction mechanisms. The values of q_e, k_A, and n_A where calculated through nonlinear regression. To prove the adequacy of the Avrami model, a function based on the normalized standard deviation was also calculated (Vieira and Pastore, 2014).

3. RESULTS AND DISCUSSION

3.1. X-ray diffraction

The X-ray diffraction profiles of MAG, Figure 1 (a), are similar to those found in the literature and present the (001) diffraction located at 5.79 ° 2θ (1.53 nm) and diffraction peaks at 11.53 ° and 17.25 ° 2θ from the (002) and (003) planes, besides peaks in the region between 24 and 30° 2θ, which are associated with the crystalline arrangement of the layers (Superti *et al*. 2007).

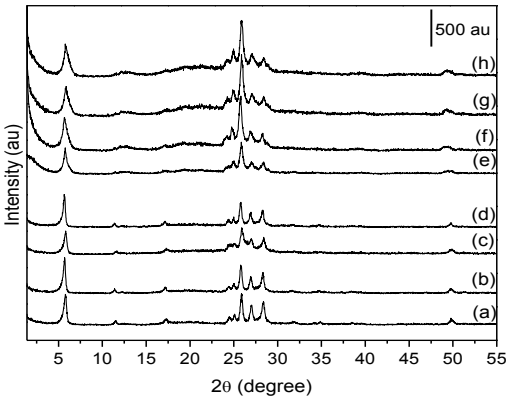

Figure 1. X-ray diffractograms of (a) MAG, MAG-PEI with (b) 10%, (c) 20%, (d) 25%, (e) 25CTA-MAG-PEI with (f) 10%, (g) 20% and (h) 25%.

The interlayer space of MAG, 1.53 nm, might be enough to allow the insertion of PEI.

The dimensions of PEI were determined with semiempirical PM6 method, and the calculations were performed with the Gaussian 09 program, D.01 version, on an idealized PEI monomer displayed in Figure 2.

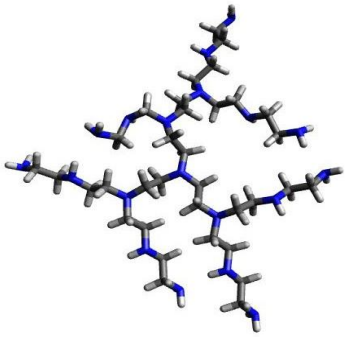

Figure 2. Monomer of polyethylenimine (PEI) calculated by PM6 method.

The larger and smaller dimensions of PEI are 2.45 and 2.15 nm, respectively. According to the literature (Wang *et al.* 2009), branched PEI chains are more flexible when the temperature increases. PEI impregnation reaction is carried out at 60 °C; therefore, although the dimensions of PEI are larger than interlayer space of MAG by *ca.* 40%, it is possible that part of PEI be accommodated into the interlayer space due to flexibility of chains. Moreover, PEI chains may also be stabilized by hydrogen bonds with silanol groups on the surface of layered silicates; in this way, the interlayer space does not change a great deal. Another part of PEI is around the layers, outside the crystals.

Figure 1 (b-d) shows MAG impregnated with PEI and the displacement of the (001) peak at 5.79° 2θ (d=1.53 nm) to 5.64° 2θ (1.57 nm) after the insertion of PEI. Furthermore, there is an overall decrease of intensity in the region between 24 and 30° 2θ assigned the presence of PEI. Figure 1 (e) presents the results of 25CTA-MAG, a weak shoulder at 2.8° 2θ, indicates the expansion of layers due to the presence of CTA^+, and suggests an increase in the basal distance from 1.53 to 3.15 nm. The low intensity of this peak is due the fact that only a part of the sodium ions was exchanged by CTA^+, however small the concentration of surfactant, it also appears the infrared spectroscopy (see later). This effect has been reported before by other authors upon the intercalation/ion exchange of surfactants in the interlayer space of layered silicates and clays (Kooli *et al.* 2006). The addition of PEI into 25CTA-MAG increases considerably the amount of organic molecules into the material; this might be the reason for the halo between 15 and 30° 2θ observed in Figure 1 (f-h). The presence of the organic portion, as large as it may be, did not seem to affect the crystalline structure these materials.

3.2. Infrared Spectroscopy

In order to evaluate the organization of bonds within a short distance in MAG as well as the modified materials, we used Fourier transform infrared spectroscopy (FTIR) in the frequency range 4000-400 cm^{-1}. Figure 2(a) shows the spectra of MAG. In the region 3800-3000 cm^{-1}, specifically bands at 3661, 3584, 3447, and 3231 cm^{-1} are associated with stretching vibrations of water and of OH groups (ν O-H) involved in interlayer hydrogen bonds and, the related bending modes at 1629 cm^{-1} (δ O-H) of different type of adsorbed water. There are also vibrations that are characteristic of magadiite: at 948 cm^{-1} attributed to the asymmetric stretching modes of terminal Si-OH.

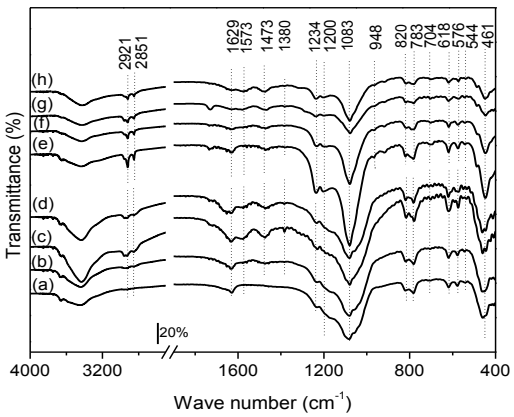

Figure 2. Fourier transform infrared spectroscopy of (a) MAG, MAG-PEI with (b) 10%, (c) 20%, (d) 25%, (e) 25CTA-MAG-PEI with (f) 10%, (g) 20% and (h) 25%.

The bands at 820 and 783 are assigned to the symmetric stretching modes of Si-O-Si

groups (silicon motions). The weak bands at 704 cm^{-1} and 690 cm^{-1} are assigned to symmetric stretching vibrations of Si-O-Si groups (coupling of Si-O stretching motions). The bands at 618, 576, and 544 are assigned to the bending modes of single and double Si-O-Si rings; their presence in the spectra indicates that the organization in the lamella is maintained (Superti *et al.* 2007).

After impregnation of PEI, Figure 2(b-d), the band at 2958 cm^{-1}, and the bands at 2927 and 2851 cm^{-1} indicate the antisymmetric and symmetric stretching, respectively. Bands at 1573 cm^{-1} are assigned to the N-H deformation in R-NH_3^+, at 1473 cm^{-1} to the scissoring vibration (δ_s CH_2) and at 1380 cm^{-1} attributed to the C-N stretching vibration were also observed, confirming that PEI was incorporated into the magadiite (MAG) (Vieira and Pastore, 2014). Figure 2(e) presents the FTIR results to confirm the presence of CTA^+ between the layers of magadiite. It is observed that, after the ion exchange, new bands at 2958 cm^{-1}, 2920 cm^{-1}, and 2851 cm^{-1} appear and are associated with the stretching vibration (ν CH), (ν_{as} CH_2), and (ν_s CH_2), respectively. Additionally, a band of bending (δ_s CH) at 1473 cm^{-1} is characteristic of methyl groups present in the polar part of the surfactant (group $N^+(CH_3)_3$), confirming the CTA^+ introduction into the interlayer space of magadiite. After impregnation of PEI, Figure 2(f-h), the vibrations observed are very similar to the ones discussed in Figure 2(b-d) and, the bands at 1573 cm^{-1} are assigned to the N-H deformation in R-NH_3^+ and, at 1473 cm^{-1} to the scissoring vibration (δ_s CH_2) confirming the PEI incorporation.

3.3. ^{13}C Solid State Nuclear Magnetic Resonance

The ^{13}C MAS NMR data for PEI-modified MAG are shown in Figure 3(a-c). The peaks at around 39 ppm (C1'), 48.5 ppm (C2'), and 52 ppm (C3') are associated with methylene groups near primary, secondary and tertiary amine groups, the secondary amines being more intense (Sayari *et al.* 2012). Furthermore, a peak around 164.7 ppm is associated with C=O from CO_2 in the carbamate ion in different interactions involving primary and secondary amines. (Sayari *et al.* 2012).

For 25CTA-MAG modified with PEI, Figure 2 (d-f), only peaks associated with carbon atoms of CTA^+ chains at 15.4 (C16), 24.3 (C3), 26.3 (C15), 28.0 (C2), 33.0 (C4-13), 53.3 (17-19) and 66.9 (C1) ppm are clearly seen (Kooli *et al.* 2006). The carbon atoms in PEI that appear at 39-48.7 ppm (C1', C2' and C3') are hardly observed. Only in 25CTA-MAG-PEI25 is it possible to identify a weak peak at 165 ppm associated with ammonium carbamate.

3.4. CHN and TG analyses

The results of PEI incorporation indicate that the amounts of PEI into MAG are close to the calculated values (10, 20 or 25 wt %). For MAG-PEI10, 20 and 25, the values are 12.1, 20.0 and 25.1%, respectively, and for 25CTA-MAG-PEI10, 20 and 25%, the values are 9.8, 17.2 and 20.9 %, respectively. For 25CTA-MAG-PEI, the loads of PEI are similar to those MAG-PEI shown above: the concentration of N is almost equal, ranging from 2.43-5.41 mmol g^{-1} in the MAG-PEI to 2.92-5.31 mmol g^{-1} in 25CTA-MAG (already discounting the N atoms coming from CTA^+) in 25CTA-MAG.

For MAG, there is a total weight loss of 11.6% between 20 and 1000 °C. The weight loss is 10.5 % at 113 and 155 °C and is associated with dehydration of the solid. There is also the weight loss of 1.1 % at 294 °C attributed to the condensation of silanols followed by a loss of water (formation of siloxanes groups) (Eypert-Blaison *et al.* 2002). MAG modified with PEI displays a weight loss between 180 and 350 °C associated with the degradation of PEI chains. For the 25CTA-MAG, there is a weight loss between 180 and 430 °C associated with the elimination of CTA^+ chains in different steps, followed by decomposition of PEI chains between 250 and 390 °C.

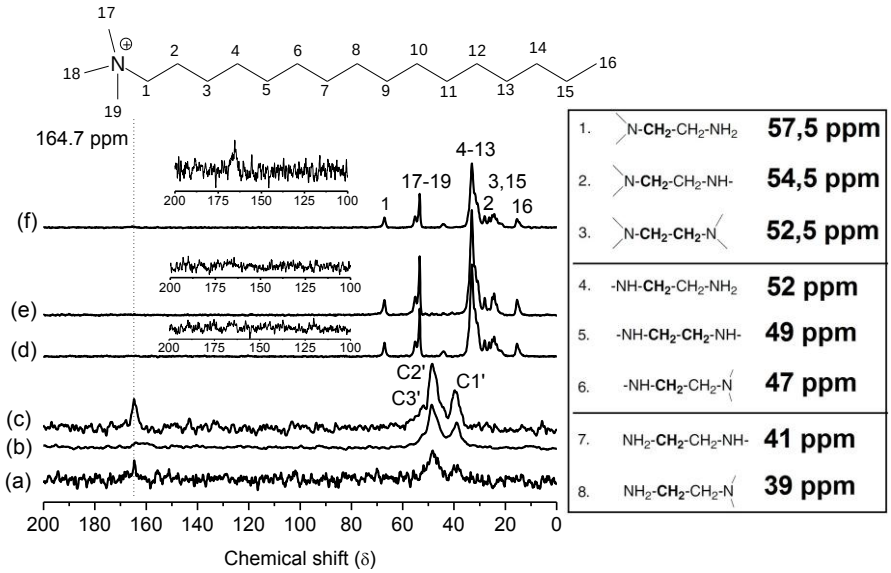

Figure 3. ^{13}C Solid state nuclear magnetic resonance of MAG-PEI with (a) 10%, (b) 20%, (c) 25% and 25CTA-MAG with (d) 10%, (e) 20% and (f) 25%.

These results suggest that the sorbents are thermally stable until 200 °C; the degradation of organic molecules present in the sorbent begins at 209 °C Thus, these sorbents were evaluated on their performance in CO_2 adsorption by CO_2-TPD experiments.

3.5. CO_2-TPD Experiments

The adsorption capacity for the prepared sorbents was evaluated by CO_2-TPD experiments; the results are shown in Figure 4 (a-g). The time of adsorption of 3 h was chosen for all experiments according to recent studies realized in our group (Vieira and Pastore, 2014) and the adsorption capacity was 2.79 mmol g^{-1} of CO_2 for MAG-PEI10 solid sorbent. For pure magadiite, MAG, Figure 4 (a), is clearly observed that no CO_2 was desorbed; only a flat baseline was obtained throughout the whole experiment. For MAG-PEIx sorbents, in Figure 4 (b-d), desorption of CO_2 begins at around 65-70 °C, with two peaks at 125-129 °C and 150 °C. For 25CTA-MAG-PEIx, in Figure 4 (e-g) the desorption of CO_2 starts at around 64-66 °C, with one peak at 130 °C for 25CTA-MAG-PEI10 and two desorption peaks at 123 °C and 150 °C for 25CTA-MAG-PEI20 and 117 °C and 146 °C to 25CTA-MAG-PEI25. These temperatures indicate that there are sites with different basicity in MAG-PEI and 25CTA-MAG-PEI.

According to the literature (Wang *et al.* 2012), there can be two sites of adsorption in PEI, the exposed PEI layer, which is responsible for the majority of CO_2 adsorbed, and bulky PEI, which contributes poorly in the adsorption and is formed by agglomeration of the polymer chains into the interlayer space and may suggest the operation of a subsurface diffusion model where, during the heating, CO_2 is removed from the exposed PEI layer by desorption leading to two events: either it is swept out from the reactor by the carrier gas or it penetrates into the subsurface region toward bulky PEI. In the other words, this diffusion model supports the existence of different paths by which CO_2 can react on the adsorbent surface. This is probably due the fact that the presence of large amounts of CTA^+ hindered the diffusion of CO_2 within the interlayer space. The hindrance of diffusion of CO_2 by CTA^+ is more evident when comparing 25CTA-MAG-PEI20 and 25CTA-MAG-PEI25 sorbents: if we take into account that the increase in PEI concentration (comparing MAG-PEI20 and MAG-PEI25), causes the increase in the adsorption capacity from 4.56 to 6.11 mmol g^{-1}, the decrease of CO_2

adsorption when CTA^+ is present in the interlayer space (from 4.57 to 3.41 mmol g^{-1}) confirms that the surfactant molecule is really causing diffusion.

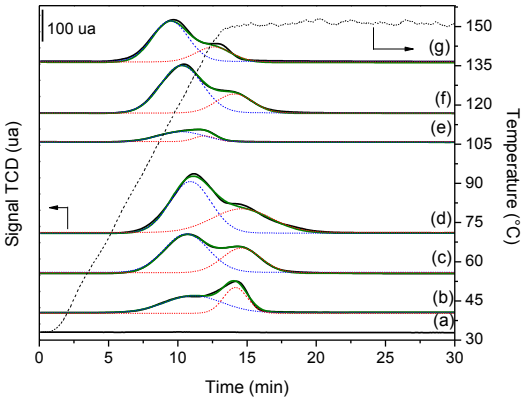

Figure 4. CO_2 Temperature programmed desorption profiles of (a) MAG, MAG-PEI with (b) 10%, (c) 20% and (d) 25%, 25CTA-MAG-PEI with (e) 10%, (f) 20% and (g) 25%.

The very similar adsorption capacities of MAG-PEI20 and 25CTA-MAG-PEI20 suggest that the limit of CTA^+ concentration without disturbance of CO_2 diffusion is up to around 20% w/w; increases of CTA^+ concentration above this range decrease the adsorption capacity of 25CTA-MAG-PEI sorbents.

3.6. Avrami Kinetic Model

Figure 5 (a-f) shows the desorption kinects for the sorbents studied here. The CO_2 desorption adsorbed is essentially complete in 15 min, indicating that short cycles can be performed to characterize the PEI-MAG nanocomposites for CO_2 adsorption. The experiments of desorption were fitted by the Avrami model and the results are presented in Table 3. The values of n_A obtained in the range of 2.77-3.77 confirm that there are different desorption mechanisms (Cestari *et al.* 2006), these can be associated with the interaction of CO_2 with primary and secondary alkyl amine groups and silanol groups. The values of k_A showed that the desorption of CO_2 from MAG-PEI was slower than that of 25CTA-MAG-PEI, suggesting that the contribution of the stronger bonded CO_2 molecules is larger in the absence of CTA^+ than in its presence. It was already commented that the presence of CTA^+ increases the concentration of CO_2 interacting with the exposed PEI layer, therefore, in a weaker interaction.

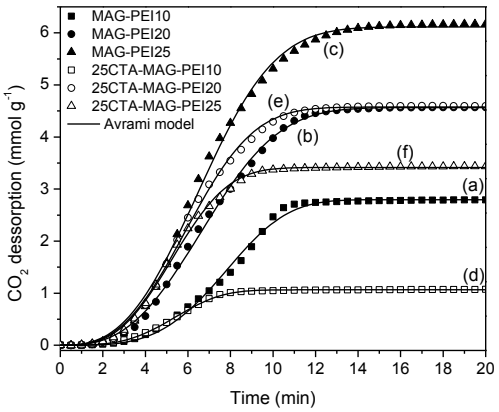

Figure 5. Desorption kinetics of MAG-PEI with (a) 10%, (b) 20% and (c) 25%, 25CTA-MAG-PEI with (d) 10%, (e) 20% and (f) 25%.

The opposite is found in the absence of CTA^+, that is, in MAG-PEI samples. This is probably the reason for the slower k_A for MAG-PEI in relation to 25CTA-MAG-PEI. The values shown in Table 3 also confirm the adequacy of the Avrami model by the low values of standard deviation (below of 8.0 %) and a correlation factor between 0.9974 and 0.9995.

Table 3. Parameters of Avrami's model adjusted to experimental data.

Sample		q_e (mmol g^{-1})	n_A	k_A (min^{-1})
MAG-PEI	10	2.79	3.77	0.12
	20	4.56	2.83	0.13
	25	6.11	2.77	0.13
25CTAMAG	10	1.06	3.49	0.17
	20	4.57	2.86	0.15
	25	3.41	3.04	0.17

4. CONCLUSION

A novel sorbent was synthesized through the impregnation of PEI into the interlayer space of layer silicate type magadiite and organo-magadiite. Magadiite has an interlayer space that can be modified as to diminish diffusional restrictions and to host variable concentration of PEI. The presence of CTA^+ surfactant in the concentration studied decreased the adsorption capacity due to the difficulty for CO_2 to access the inner sites of adsorption; however the access of CO_2 to layered PEI was improved. Moreover, they displayed high thermal stability and fast kinetics of desorption and may be submitted to adsorption/desorption cycles. The Avrami model proved to be a good kinetic model to describe the interaction of CO_2 with PEI impregnated in layered silicates.

5. ACKNOWLEDGMENTS

To PETROBRAS for the financial support to this work as well as for the fellowship to R.B.V. The authors are indebted to Prof. Lucas Ducati for his work in calculating the dimensions of PEI.

6. REFERENCES

CESTARI, A. R.; VIEIRA, E. F. S.; VIEIRA, G. S.; ALMEIDA, L. E. The removal of anionic dyes from aqueous solutions in the presence of anionic surfactant using aminopropylsilica—A kinetic study. *J. Hazard. Mater. B*, v. 138, p. 133−141, 2006.

CHOI, S.; DRESE, J. H.; JONES, C. W. Adsorbent materials for carbon dioxide capture from large anthropogenic point sources. *ChemSusChem*, v. 2, p. 796−854, 2009.

EUGSTER, H. P. Hydrous sodium silicates from lake Magadi, Kenya: Precursors of bedded chert. *Science*, v. 157, p. 1177−1180, 1967.

EYPERT-BLAISON, C.; MICHOT, L. J.; HUMBERT, B.; PELLETIER, M.; VILLIÉRAS, F.; CAILLERIE, J.-B. d'E. Hydration water and swelling behavior of magadiite. the H^+, Na^+, K^+, Mg^{2+}, and Ca^{2+} exchanged forms. *J. Phys. Chem. B*, v. 106, p. 730−742, 2002.

KINEFUCHI, I.; YAMAGUCHI, H.; SAKIYAMA, Y.; TAKAGI, S.; MATSUMOTO, Y. Inhomogeneous decomposition of ultrathin oxide films on Si(100): Application of Avrami kinetics to thermal desorption spectra. *J. Chem. Phys.* v. 128, p. 164712−6, 2008.

KOOLI, F.; MIANHUI, L.; ALSHAHATEET, S. F.; CHEN, F.; YINGHUAI, Z. Characterization and thermal stability properties of intercalated Na-magadiite with cetyltrimethylammonium (C16TMA) surfactants *J. Phys. Chem. Solids*, v. 67, p. 926−931, 2006.

SAMANTA, A.; ZHAO, A.; SHIMIZU, G. K. H.; SARKAR, P.; GUPTA, R. Post-combustion CO_2 capture using solid sorbents: A review. *Ind. Eng. Chem. Res.* v. 51, p. 1438−1463, 2012.

SAYARI, A.; HEYDARI-GORJI, A.; YANG, Y. CO_2-Induced degradation of amine-containing adsorbents: Reaction products and pathways. *J. Am. Chem. Soc.* v. 134, p. 13834−13842, 2012.

SUPERTI, G. B.; OLIVEIRA, E. C.; PASTORE, H. O.; BORDO, A.; BISIO, C.; MARCHESE, L. Aluminum magadiite: An acid solid layered material. *Chem. Mater.* v. 19, p. 4300−4315, 2007.

VIEIRA, R. B; PASTORE, H. O. Polyethylenimine-magadiite layered silicate sorbent for CO_2 capture. *Environ. Sci. Technol.* v. 48, p. 2472-2480, 2014.

VON HARPE, A.; PETERSEN, H.; LI, Y.; KISSEL, T. Characterization of commercially available and synthesized polyethylenimines for gene delivery. *J. Controlled Release*, v. 69, p. 309−322, 2000.

WANG, X.; SCHWARTZ, V.; CLARK, J. C.; MA, X.; OVERBURY, S. H.; XU, X.; SONG, C. Infrared study of CO_2 sorption over "molecular basket" sorbent consisting of polyethylenimine-modified mesoporous molecular sieve. *J. Phys. Chem. C*, v. 113, p. 7260−7268, 2009.

WANG, X.; MA, X.; SCHWARTZ, V.; CLARK, J. C.; OVERBURY, S. H.; ZHAO, S.; XU, X.; SONG, C. A solid molecular basket sorbent for CO_2 capture from gas streams with low CO_2 concentration under ambient conditions. *Phys. Chem. Chem. Phys.* v. 14, p. 1485−1492, 2012.

XU, X.; SONG, C.; ANDRESEN, J. M.; MILLER, B. G.; SCARONI, A. W. Novel polyethylenimine-modified mesoporous molecular sieve of MCM-41 type as high-capacity adsorbent for CO_2 capture. *Energy Fuels*, v. 16, p. 1463−1469, 2002.